Tracing Cosmic Evolution with Galaxy Clusters
ASP Conference Series, Vol. 268, 2002
S. Borgani, M. Mezzetti, and R. Valdarnini, eds.

Discovery of Holes in the Core of the Distant Galaxy Cluster RBS797 in a CHANDRA Observation

E. De Filippis

Astrophysics Research Institute (Liverpool John Moores University)

S. Schindler (1), A. Castillo-Morales (1), A. Schwope (2),
J. Wambsganss (3)

(1) Astrophysics Research Institute (Liverpool John Moores University), (2) Astrophysikalisches Institut Potsdam, (3) Universität Potsdam, Institut für Physik

Abstract. We present CHANDRA X-ray observations of the hot ($T = 7.7^{+1.2}_{-1.0}$), distant ($z = 0.354$) galaxy cluster RBS797. The most striking features are two spectacular minima in the X-ray emission in the core of the cluster; this suggests an interaction of radio lobes with the intracluster gas. This is the first time such depressions have been observed in a distant cluster.

1. Introduction

In this poster we present the final results of the analysis of the galaxy cluster RBS797. RBS797 has been observed by the CHANDRA Advanced CCD Imaging Spectrometer (ACIS) I detector on October 20^{th}, 2000 for a total exposure time of 13.3 *ksec*.
Throughout this poster we have used: $H_0 = 50\ km \cdot s^{-1} \cdot Mpc^{-1}$ and $q_0 = 0.5$ and errors, if not otherwise specified, are 90% confidence levels.

2. General characteristics

A CHANDRA image of the centre of the cluster in the $0.5 - 7.0\,keV$ energy band, smoothed with a Gaussian filter of $\sigma = 0.75\,arcsec$, is shown in the left panel in Figure 1.
RBS797 shows a slightly elliptical X-ray morphology. The most spectacular features are two minima in the X-ray emission of about $20 - 30\,kpc$ in size; these minima are located opposite to each other with respect to the cluster centre (ENE and WSW direction), and at a distance of about $5\,arcsec$ from the cluster centre.
The central morphology of the cluster, with its depressions in the X-ray surface brightness, is similar to the one of Perseus cluster (Fabian et al. 2000) and of Hydra-A (McNamara et al. 2000), with the difference that in RBS797 the two holes are even more pronounced. Cuts in direction of the minima in the

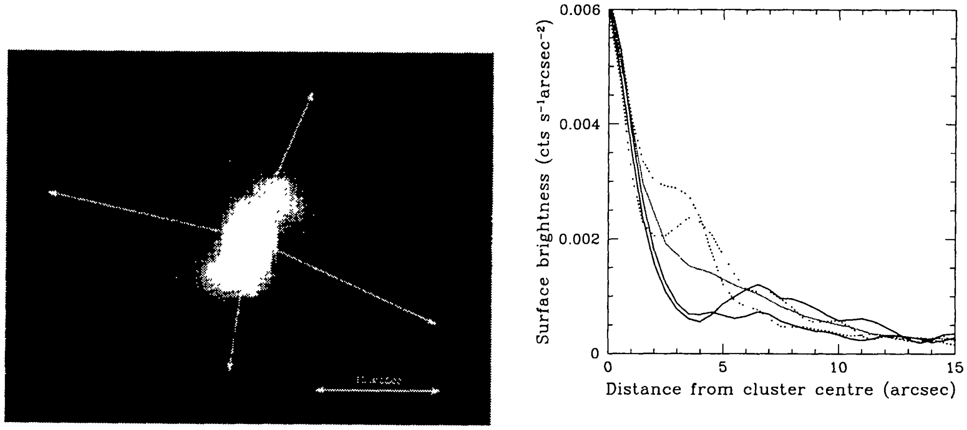

Figure 1. **Left panel**: CHANDRA image of the central 35 $arcsec^2$ of the cluster RBS797. **Right panel**: Traces of the X-ray emission from the cluster centre in direction of the minima (solid lines, position angles 77° and 246°), in the perpendicular direction (dotted lines, position angles 172° and 337°) and the average for the whole cluster (red line).

X-ray emission (solid lines) and in direction perpendicular to it (dotted lines) are plotted in the right panel in Fig. 1 (for reference in the directions of the cuts also see the left panel); the red line in the right panel shows an X-ray emission profile averaged for the whole cluster centre. We can estimate an X-ray deficit of a factor of approximately $3 - 4$ in the holes, compared to the perpendicular directions where the gas is probably compressed. These features suggest an interaction of the central cluster galaxy with the intra-cluster medium. This is the first discovery of such holes in a *distant cluster*.

3. Spectral analysis

The CHANDRA data have then been used to derive the temperature and metallicity of RBS797. The results of the spectral analysis are summarised in Table 1. We treat the central point-like source (radius $\leq 2\,arcsec$), probably an AGN, separately, because it would distort the thermal spectrum of the intra-cluster gas. The source has a count rate of about $0.026\,cts/s$ and a flux $F(2-10\,keV) = 2.2 \times 10^{-13} erg/s/cm^2$. The spectrum is vary flat; a power law yields a good fit with a very law index of 1.2 ± 0.2.
The cluster overall emission is well fit by a model with a relative high temperature of $T = 7.7keV$ and a metallicity of 0.26 in solar units. The X-ray luminosity is $L_X(0.5 - 7.0keV) = 4.0 \times 10^{45} erg \cdot s^{-1}$ and $L_X(bol) = 6.7 \times 10^{45} erg \cdot s^{-1}$.
The cluster has then been subdivided into three annuli in order to get an estimation of its radial temperature profile. The result is shown in the left panel in Figure 2; a trend is observed of increasing temperature with the radius, but the results are almost consistent with constant values. In the figure are also shown, in dotted lines, the confidence limits of the mean ambient cluster temperature.

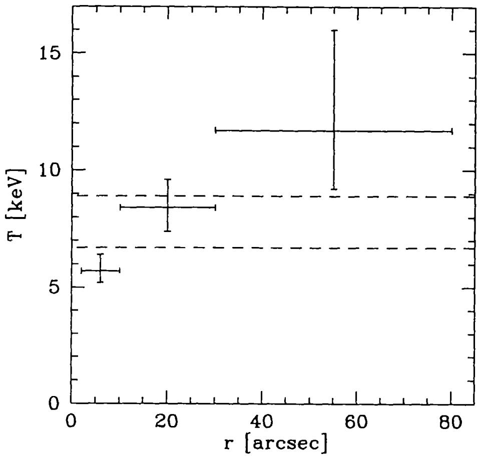

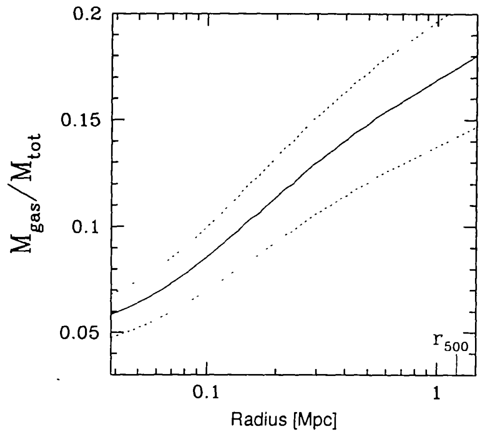

Figure 2. **Left panel**: Radial projected X-ray gas temperature profile. Horizontal error bars show the boundaries of the annuli. The dotted lines mark the 90% confidence region of the mean ambient cluster temperature. **Right panel**: ratio of the X-ray gas mass to total gravitating mass as a function of radius. The three lines show the best-fit value (solid line) and conservative confidence limits (dotted lines).

A spectral analysis of the bright *arms* surrounding the minima has been performed separately: their emission comes mainly from *soft* X-rays. With 1387 source counts extracted from these regions, a temperature of $4.4\,keV$, lower than for the rest of the cluster, is found, implying that these can not be shocked regions.

The X-ray surface brightness profile of RBS797 can be fitted well by a β model (Cavaliere & Fusco-Femiano 1976) when ignoring the central source: $\beta = 0.63 \pm 0.01$, $r_c = 8.1 \pm 0.6\,arcsec$ and a central surface brightness $S_0 = 6.6\,cts/s/arcmin^2$. Assuming a spherical symmetry, this corresponds to a gas mass $M_{gas}(r_{500}) = 1.13(\pm 0.09) \times 10^{14} M_\odot$, with $r_{500} = 1.22(\pm 0.08)$Mpc. Assuming also hydrostatic equilibrium, the total mass of the cluster can be estimated. For an isothermal cluster of $T = 7.7\,keV$ the total mass is $M_{tot}(r_{500}) = 6.5^{+1.6}_{-1.2} \times 10^{14} M_\odot$. This corresponds to a gas mass fraction $f_{gas}(r_{500}) = 0.17^{+0.06}_{-0.05}$ which is in good agreement with the gas mass fractions found in samples of nearby and distant clusters (Ettori & Fabian 1999; Schindler 1999). For this cluster we find an increasing gas mass fraction (see Figure 2, right panel) implying that the gas distribution is more extended than the dark matter.

4. Summary and conclusions

RBS797 appears as a slightly elliptical, hot cluster with the gas temperature slightly increasing outward with the radius. Two strongly pronounced depressions are present in the X-ray emission, having diameters of $20 - 30\,kpc$ and with a factor of $3 - 4$ less emission that in the other directions. The low temperature of the regions surrounding the holes is a clear indication that these cannot be

Table 1. Column (1) shows the radii, in arc-seconds, of the regions from which the photons have been extracted. Col.(2): model used for the fit: MeKaL = Kaastra & Mewe (1993), Liedahl, Osterheld & Goldstein (1995), PL = power law. Col.(3): energy range in keV. In columns (4-6) the fit parameters are given: temperature in keV (for PL fit is the power law index), metallicity in solar units, redshift. Col.(7): reduced χ^2. The hydrogen column density is fixed to the Galactic value (Dickey & Lockman 1990).

Radius	Model	En. range	kT	Metallicity	Redshift	$\frac{\chi^2}{d.o.f.}$
2 – 80	MeKaL	0.5 – 10	$7.7^{+1.2}_{-1.0}$	0.26 ± 0.10	0.39 ± 0.02	1.2
2 – 80	MeKaL	2 – 10	$7.1^{+1.6}_{-1.5}$	0.25 ± 0.12	0.39 ± 0.02	1.0
2 – 80	MeKaL	2 – 10	$7.4^{+1.7}_{-1.1}$	0.17 ± 0.11	0.354(fixed)	0.9
2 – 10	MeKaL	0.5 – 10	$5.7^{+0.7}_{-0.5}$	$0.38^{+0.17}_{-0.16}$	0.39(fixed)	1.6
10 – 30	MeKaL	0.5 – 10	$8.4^{+1.2}_{-1.0}$	0.25 ± 0.18	0.39(fixed)	1.0
30 – 80	MeKaL	0.5 – 10	$11.7^{+4.3}_{-2.5}$	$0.20^{+0.35}_{-0.20}$	0.39(fixed)	1.2
arms	MeKaL	0.5 – 10	$4.4^{+0.7}_{-0.6}$	0.26(*fixed*)	0.39(fixed)	1.2
0 – 2	PL	0.5 – 10	1.2 ± 0.2	-	0.39(fixed)	0.9
0 – 2	0.59× MeKaL +0.41 *PL*	0.5 – 10	7.7 (fixed) 1.1 ± 0.2	0.26 (fixed)	0.39(fixed)	0.9

shock regions; it is likely that the intra-cluster gas has been subsonically pushed away from the areas of low X-ray emission to the areas of higher emission by the pressure of the relativistic particles in radio lobes.
In the next months planned follow-up radio data will hopefully give a clearer picture of the internal structure of this cluster and of the interaction of the cluster active galaxy with the intracluster medium.

References

Cavaliere, A. & Fusco-Femiano, R. 1976, A&A, 49, 137
Dickey, J.M. & Lockman, F.J. 1990, ARA&A, 28, 215
Ettori, S. & Fabian, A.C. 1999, MNRAS, 305, 834
Fabian, A.C. et al. 2000, MNRAS, 318, 65
Kaastra, J.S. & Mewe, R. 1993, A&AS, 97,443
Liedahl, D.A., Osterheld, A.L. & Goldstein, W.H. 1995, ApJ, 438, 115
McNamara, B.R. et al. 2000, ApJ, 534, 135
Schindler, S. 1999, A&A, 349, 435
Schindler, S. et al. 2001, accepted by A&AL